Restoring early postnatal synaptic dysregulation rescues motor neuron degeneration in a mouse model of Spinal and Bulbar Muscular Atrophy

Tomoki Hirunagi, Kentaro Sahashi, Madoka Iida, Kazunari Onodera, Satoshi Yokoi, Yosuke Ogura, Genki Tohnai, Kenji Sakakibara, Kentaro Maeda, C. Frank Bennett, Yohei Okada, Masahisa Katsuno

Supplementary Tables

Supplementary Table 1. Primers used for quantitative PCR analyses.
Supplementary Table 2. Base sequence and chemistry of ASOs used in this study.

Supplementary Figures

Supplementary Fig. 1. Nuclear accumulation of AR in male neonatal AR-24Q mice.
Supplementary Fig. 2. Expression of androgen receptor in motor neurons.
Supplementary Fig. 3. Effects of 5 μg AR-ASO on the expression and protein levels in the spinal cord of AR-97Q mice at P14.
Supplementary Fig. 4. Effect of Intracerebroventricular injection of 2.5 μg AR-ASO or Control-ASO on disease progression in AR-97Q mice.
Supplementary Fig. 5. Effect of intracerebroventricular injection of 5 μg AR-ASO or Control-ASO on wild-type mice.
Supplementary Fig. 6. Neonatal testosterone administration accelerates the disease phenotype of AR-97Q mice.
Supplementary Fig. 7. Gene set analysis of transcriptome data from the mouse spinal cord.
Supplementary Fig. 8. REST target glutamatergic synaptic genes are upregulated in the early stages of AR-97Q mice.
Supplementary Fig. 9. Single-nucleus RNA sequencing in the spinal cord of AR-97Q and AR-24Q mice.
Supplementary Fig. 10. Neonatal testosterone administration inhibits the expression of genes related to motor neuron maturation.
Supplementary Fig. 11. Increase in nuclear c-Fos-positive ratio in the motor neurons AR-97Q mice.
Supplementary Fig. 12. Nuclear localization of AR in iPSC-derived motor neurons.
Supplementary Fig. 13. Interaction of REST with AR-24Q and AR-97Q and effects of AR-24Q and AR-97Q on the expression of *Rest* and *Rest4* in NSC-34 cells.
Supplementary Fig. 14. Screening of ASOs targeting a micro exon in *Rest4*.
Supplementary Fig. 15. ASO-mediated splice switch from *REST4* to *REST* attenuates motor neuron hyperexcitability.
Supplementary Fig. 16. Early postnatal treatment reduces neuropeptide expression in later stages in AR-97Q mice.

Supplementary Table 1. Primers used for quantitative PCR analyses.

Gene	Forward	Reverse
Human *AR*	5′-CGGAAGCTGAAGAAACTTGG-3′	5′-ATGGCTTCCAGGACATTCAG-3′
Mouse *Ar*	5′-GGACCATGTTTTACCCATCG-3′	5′-CGTTTCTGCTGGCACATAGA-3′
Grin1	5′-AGAGCCCGACCCTAAAAAGAA-3′	5′-CCCTCCTCCCTCTCAATAGC-3′
Gria1	5′-AAAGGAGTGTACGCCATCTT-3′	5′-TGTCAACGGGAAAACTTGGA-3′
Kcng4	5′-AGTGCTATTACATCTTCGTGGTG-3′	5′-GCGACACATAGTATGGGGAGA-3′
Rab37	5′-CCAACCAGTCCTCTTTTGACAA-3′	5′-GCCTAGAAGCATAATCACCACG-3′
Tmod1	5′-TGAGCTAGATGAACTAGACCCTG-3′	5′-CGGTCCTTAAATTCCTTCGCTTG-3′
Mouse *Rest*	5′-GGCTGAAAACGAGTCTCAGG-3′	5′-TGACGTAGCTTCTGGTGGTG-3′
Mouse *Rest4*	5′-AACGCCCGTATAAATGTGAA-3′	5′-TCACCCAGCTAGATCACACT-3′
Human *REST*	5′-GGCAGCAAATGAGTCTCAGG-3′	5′-TCTGCTAGATTCTTGTGGAA-3′
Human *REST4*	5′-ACTCATACAGGAGAACGCCCA-3′	5′-GGCTTCTCACCCATCTAGATCAC-3′
Human *B2M*	5′-GAGGCTATCCAGCGTACTCCA-3′	5′-CGGCAGGCATACTCATCTTTT-3′
Human *GRIN1*	5′-ACCCCAAGATCGTCAACATTG-3′	5′-GGCTAACTAGGATGGCGTAGA-3′
Human *GRIA1*	5′-TGCTTTGTCGCAACTCACAGA-3′	5′-GGCATAGACTCCTTTGGAGAAC-3′
Uts2	5′-GTCCCAGCACTGAGACTCC-3′	5′-CCGTGTTGCTTATGTTGTTTCC-3′
Calca	5′-CAGTGCCTTTGAGGTCAATCT-3′	5′-CCAGCAGGCGAACTTCTTCTT-3′
Vip	5′-AGTGTGCTGTTCTCTCAGTCG-3′	5′-GCCATTTTCTGCTAAGGGATTCT-3′
B2m	5′-CTGACCGGCCTGTATGCTAT-3′	5′-CCGTTCTTCAGCATTTGGAT-3′

Supplementary Table 2. Base sequences and chemistries of ASOs used in this study.

ID	Base sequence	Chemistry
AR-ASO	5′-AAGTTGTAGTAGTCGC-3′	5′-kekeddddddddekek-3′
Control-ASO	5′-GGCCAATACGCCGTCA-3′	5′-kkkddddddddddkkk-3′
Rest4-ASO #1	5′-ACTCTAGTAAATATTACC-3′	5′-eeeeeeeeeeeeeeeeee-3′
Rest4-ASO #2	5′-ATCACACTCTAGTAAATA-3′	5′-eeeeeeeeeeeeeeeeee-3′
Rest4-ASO #3	5′-GCTAGATCACACTCTAGT-3′	5′-eeeeeeeeeeeeeeeeee-3′
Rest4-ASO #4	5′-ACCCAGCTAGATCACACT-3′	5′-eeeeeeeeeeeeeeeeee-3′
Rest4-ASO #5	5′-TACATACCCAGCTAGATC-3′	5′-eeeeeeeeeeeeeeeeee-3′
Rest4-ASO #6	5′-CTGAATACATACCCAGCT-3′	5′-eeeeeeeeeeeeeeeeee-3′
Rest4-ASO #7	5′-TCTACCTGAATACATACC-3′	5′-eeeeeeeeeeeeeeeeee-3′
ASO#2 scramble	5′-GCATATAATCTAATCCAA-3′	5′-eeeeeeeeeeeeeeeeee-3′
ASO#3 scramble	5′-ATCCTGAATATACGCGTC-3′	5′-eeeeeeeeeeeeeeeeee-3′
hREST4-ASO	5′-CACACTCTAGTAAATATTAC-3′	5′-eeeeeeeeeeeeeeeeeeee-3′
hScramble-ASO	5′-GAAACTATCAATCTCTCATA -3′	5′-eeeeeeeeeeeeeeeeeeee-3′

k: cEt, e: 2′-MOE, d: DNA

ASOs with a phosphorothioate backbone and all 5-methylcytosines were used in this study

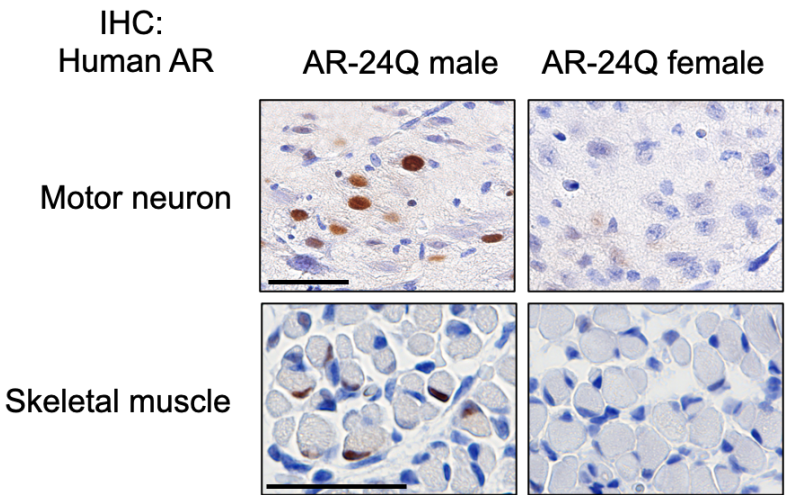

Supplementary Fig. 1 Nuclear accumulation of AR in male neonatal AR-24Q mice.
Anti-human androgen receptor (AR) immunostaining of motor neurons and skeletal muscles of male and female AR-24Q mice at postnatal day 1. Representative images are shown. Similar results were obtained in three independent experiments. Scale bar = 50 μm.

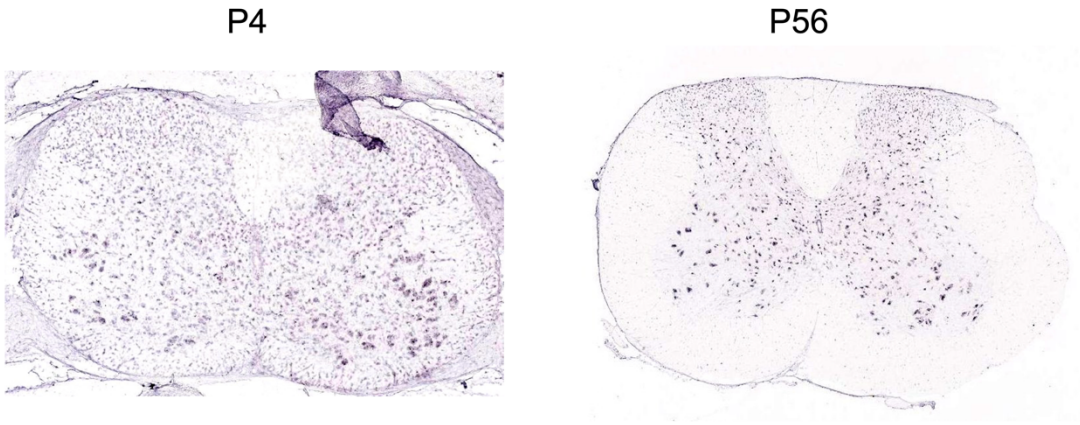

Image credit : Allen Institute

Supplementary Fig. 2 Expression of *androgen receptor* in motor neurons.
In situ hybridization images from Allen Spinal Cord Atlas show *androgen receptor* expression in motor neurons of the anterior horn of the mouse spinal cord at P4 and P56.

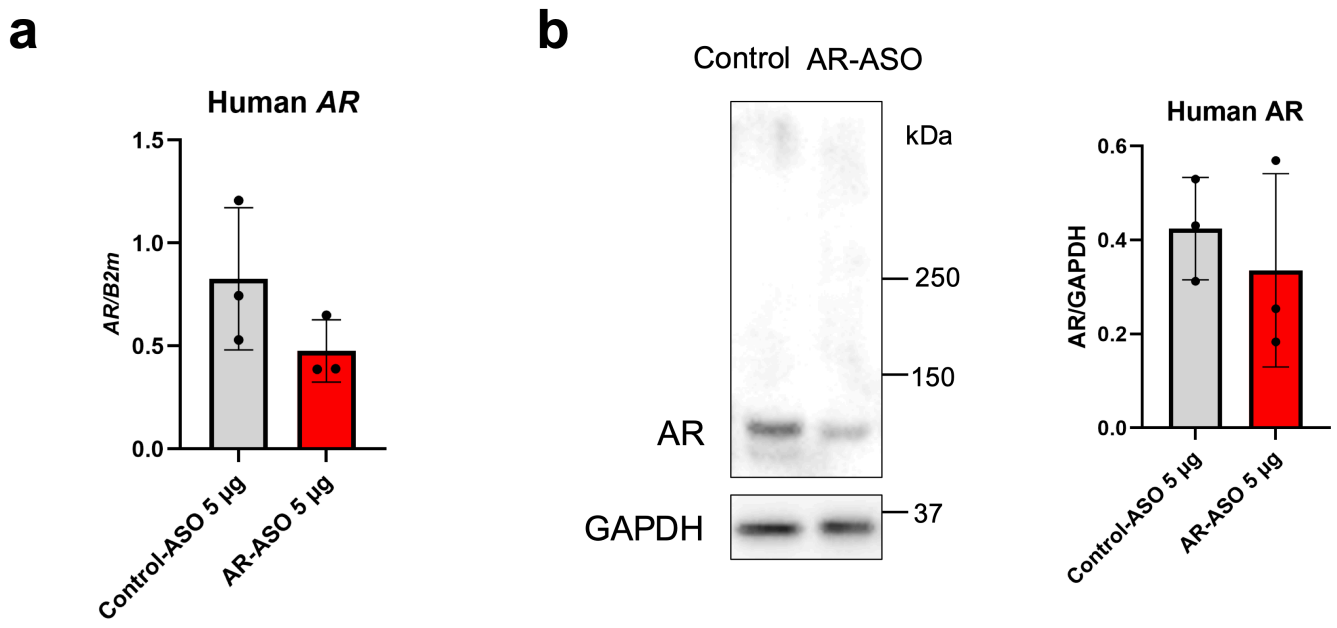

Supplementary Fig. 3 Effects of 5 μg AR-ASO on the mRNA expression and protein levels in the spinal cord of AR-97Q mice at P14.
a qPCR analysis of human androgen receptor (*AR*) mRNA normalized to *beta-2-microglobulin* (*B2m*) in the spinal cord of Control-ASO (5 μg) or AR-ASO (5 μg) injected AR-97Q mice at P14 (n = 3 mice/group). **b** Immunoblots for human AR of the spinal cord of Control-ASO (5 μg) or AR-ASO (5 μg) injected AR-97Q mice at P14 (n = 3 mice/group). Data are presented as mean values +/- SD. Significance was tested by two-tailed unpaired *t*-test for the two group comparisons. Source data are provided as a Source Data file.

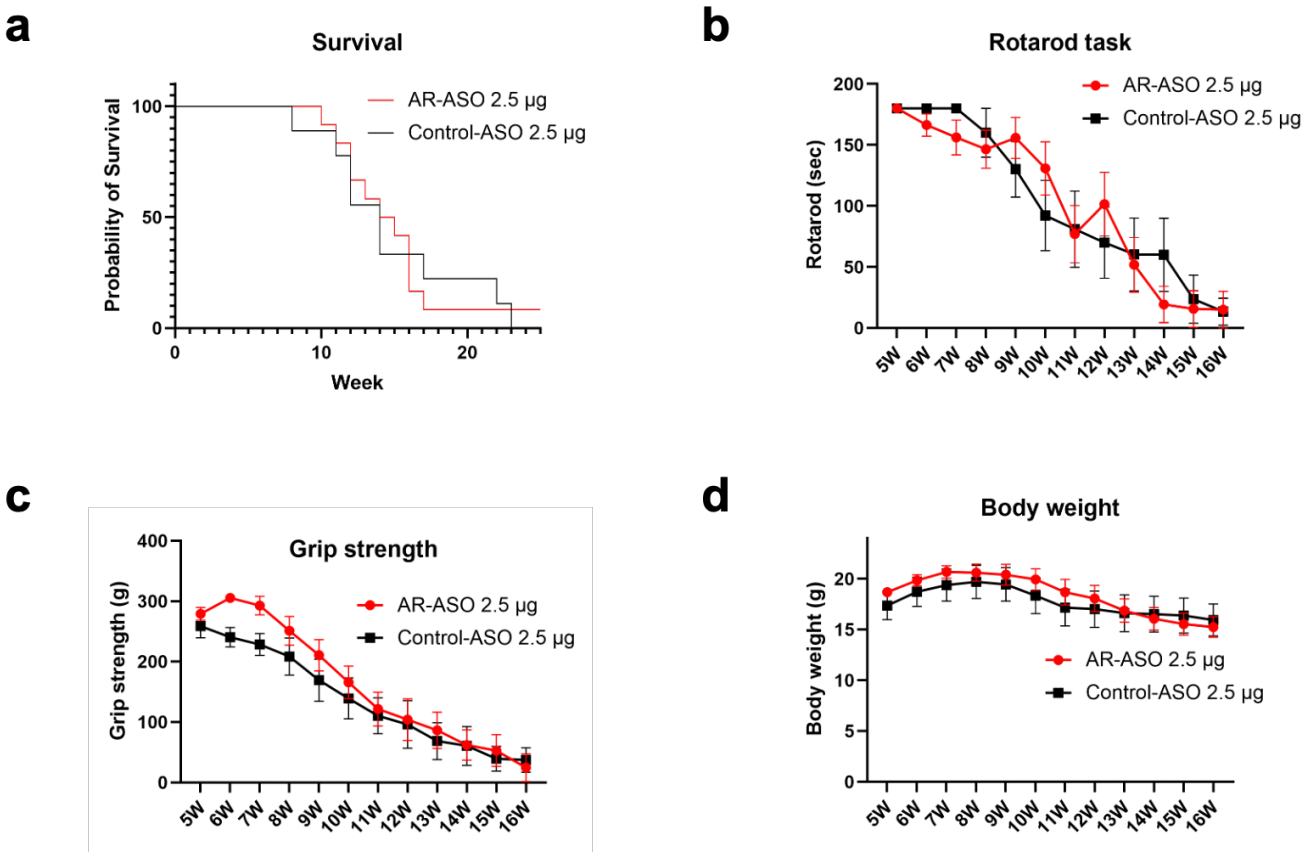

Supplementary Fig. 4 Effect of intracerebroventricular injection of 2.5 μg AR-ASO or Control-ASO on disease progression in AR-97Q mice.
a–d AR-ASO (n = 12) or Control-ASO (n = 9) at the dose of 2.5 μg was intracerebroventricularly injected to male AR-97Q mice at P1. Survival (**a**), rotarod performance (**b**), grip strength (**c**), and body weight (**d**) of the mice were shown. Data are presented as mean values +/- SEM (**b–d**). Source data are provided as a Source Data file.

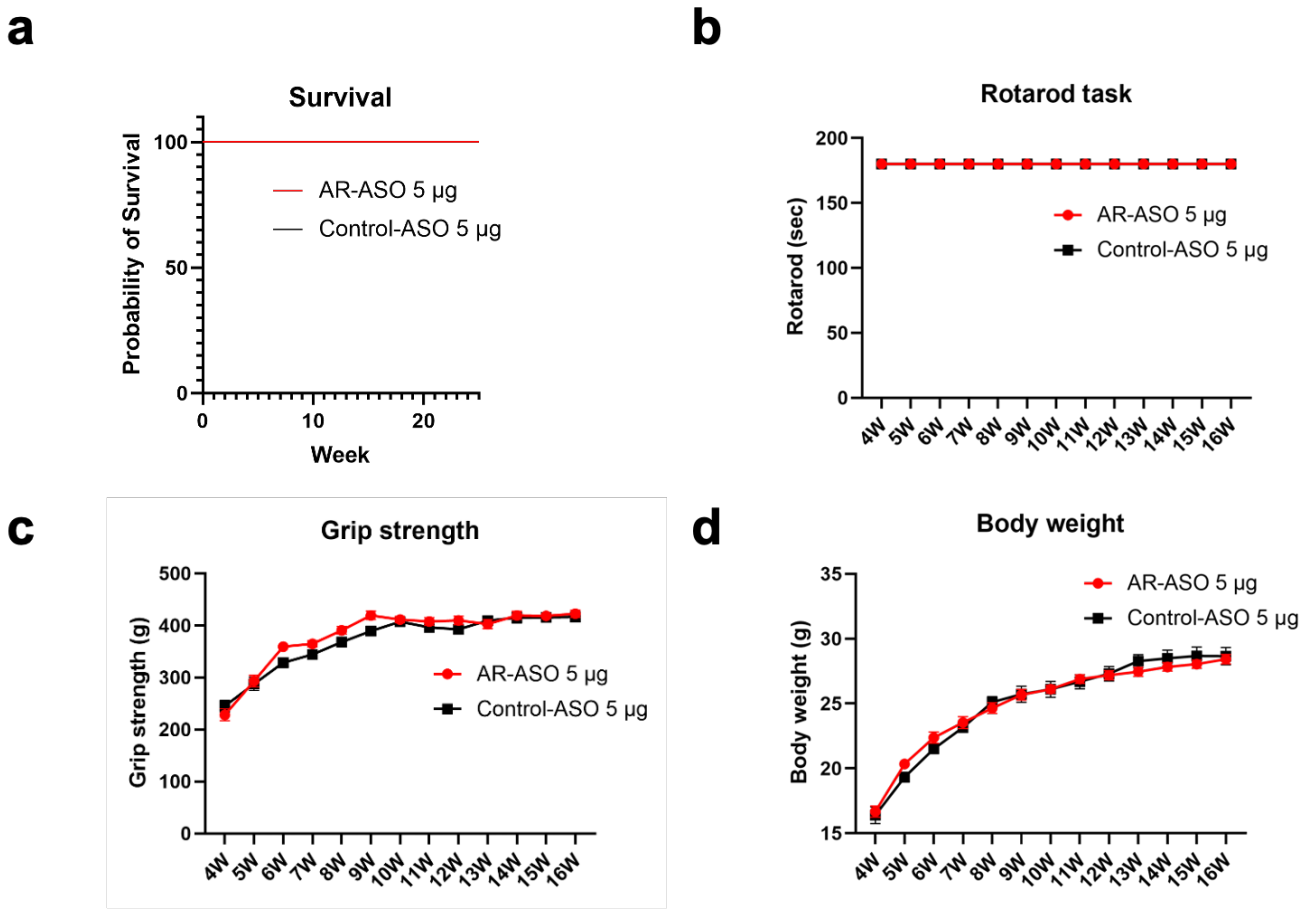

Supplementary Fig. 5 Effect of intracerebroventricular injection of 5 μg AR-ASO or Control-ASO on wild-type mice.
a–d AR-ASO or Control-ASO at the dose of 5 μg was intracerebroventricularly injected to male wild-type mice at P1 (n = 10 mice/group). Survival (**a**), rotarod performance (**b**), grip strength (**c**), and body weight (**d**) of the mice were shown. Data are presented as mean values +/- SEM (**b–d**). Source data are provided as a Source Data file.

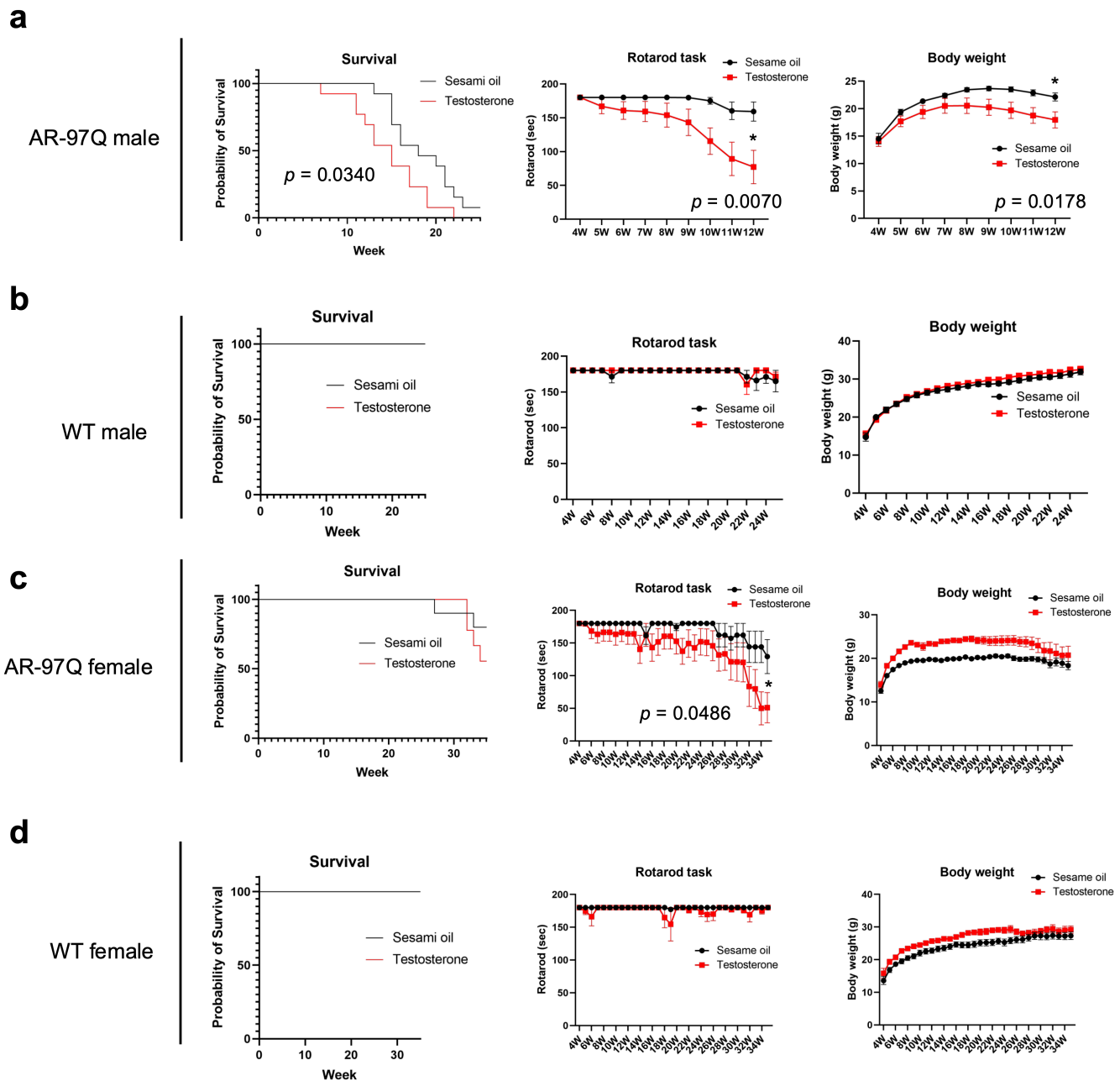

Supplementary Fig. 6 Neonatal testosterone administration accelerates the disease phenotype of AR-97Q mice.

a–d At postnatal day1, 20 μg of testosterone or sesame oil vehicle was subcutaneously administered to male AR-97Q (n = 13 mice per group), male wild-type (WT) (n = 11 and 8 mice, respectively), female AR-97Q (n = 9 and 10 mice, respectively), and female WT mice (n = 6 and 8 mice, respectively). Survival, rotarod performance, and body weight were shown. Data are presented as mean values +/- SEM. Significance was tested by log-rank test for the survival rate, two-tailed Mann-Whitney test for rotarod task at 12 or 35 weeks of age (**a**,**c**), and two-tailed unpaired *t*-test for body weight at 12 weeks of age (**a**). Source data are provided as a Source Data file.

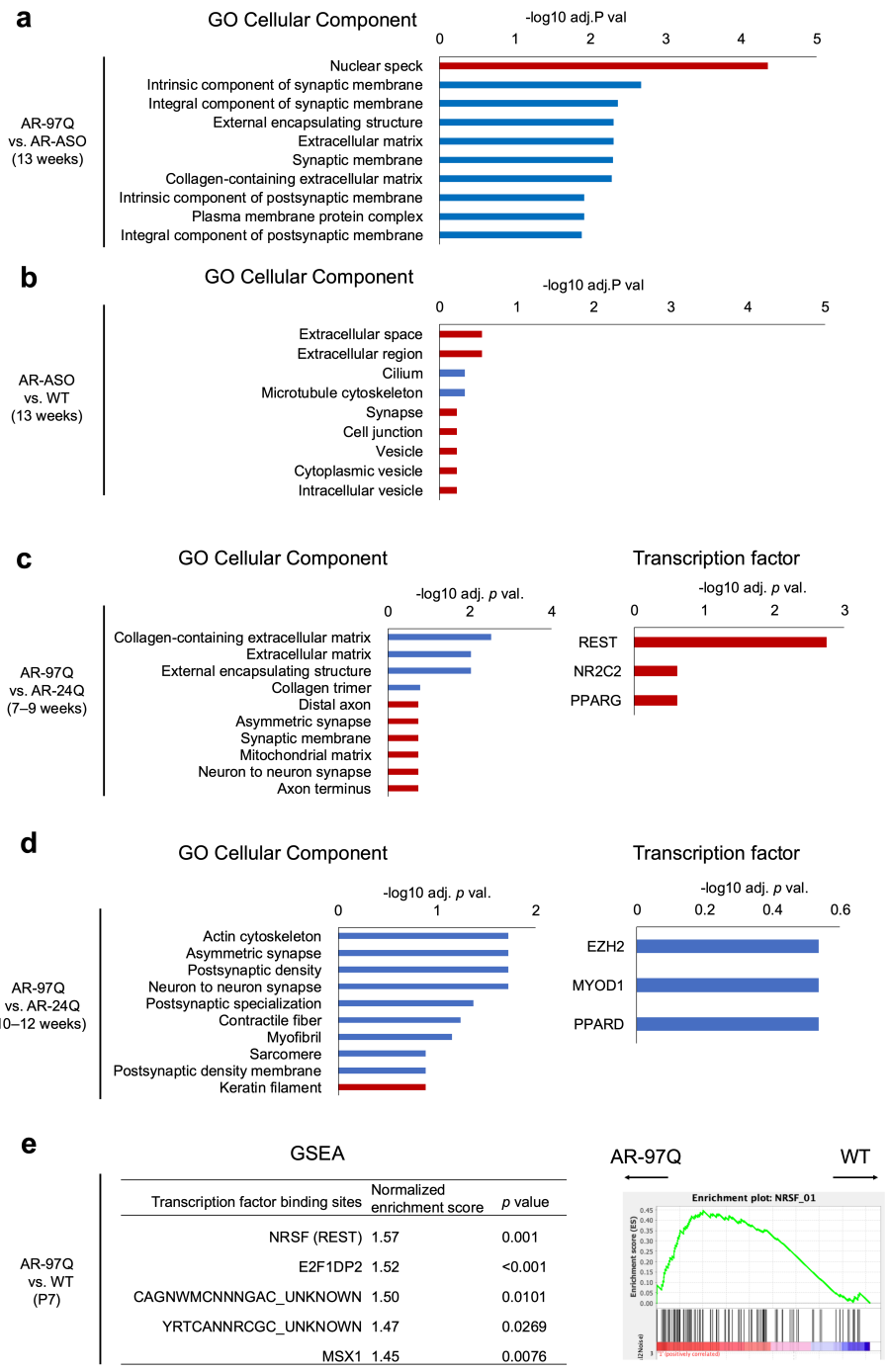

Transcription factor binding sites	Normalized enrichment score	*p* value
NRSF (REST)	1.57	0.001
E2F1DP2	1.52	<0.001
CAGNWMCNNNGAC_UNKNOWN	1.50	0.0101
YRTCANNRCGC_UNKNOWN	1.47	0.0269
MSX1	1.45	0.0076

Supplementary Fig. 7 Gene set analysis of transcriptome data from the mouse spinal cord. **a,b** Generally Applicable Gene-set Enrichment (GAGE) analysis of RNA-seq data from the spinal cord of AR-97Q and AR-ASO-treated AR-97Q mice (**a**) and AR-ASO-treated AR-97Q and wild-type (WT) mice (**b**) at 13 weeks of age (n = 3 mice/group). **c,d** GAGE analysis of microarray data from the spinal cord of AR-97Q and AR-24Q mice at 7–9 weeks (**c**) and 10–12 weeks (**d**) of age (n = 3 mice/group). **e** Gene Set Enrichment Analysis (GSEA) of RNA-seq data from the spinal cord of AR-97Q and WT mice at P7 in the category of “transcription factor targets”. Top five transcription factor binding sites and the enrichment plot of neuron-restrictive silencer factor (NRSF) were shown. NRSF is an alternative name for REST. Source data are provided as a Source Data file.

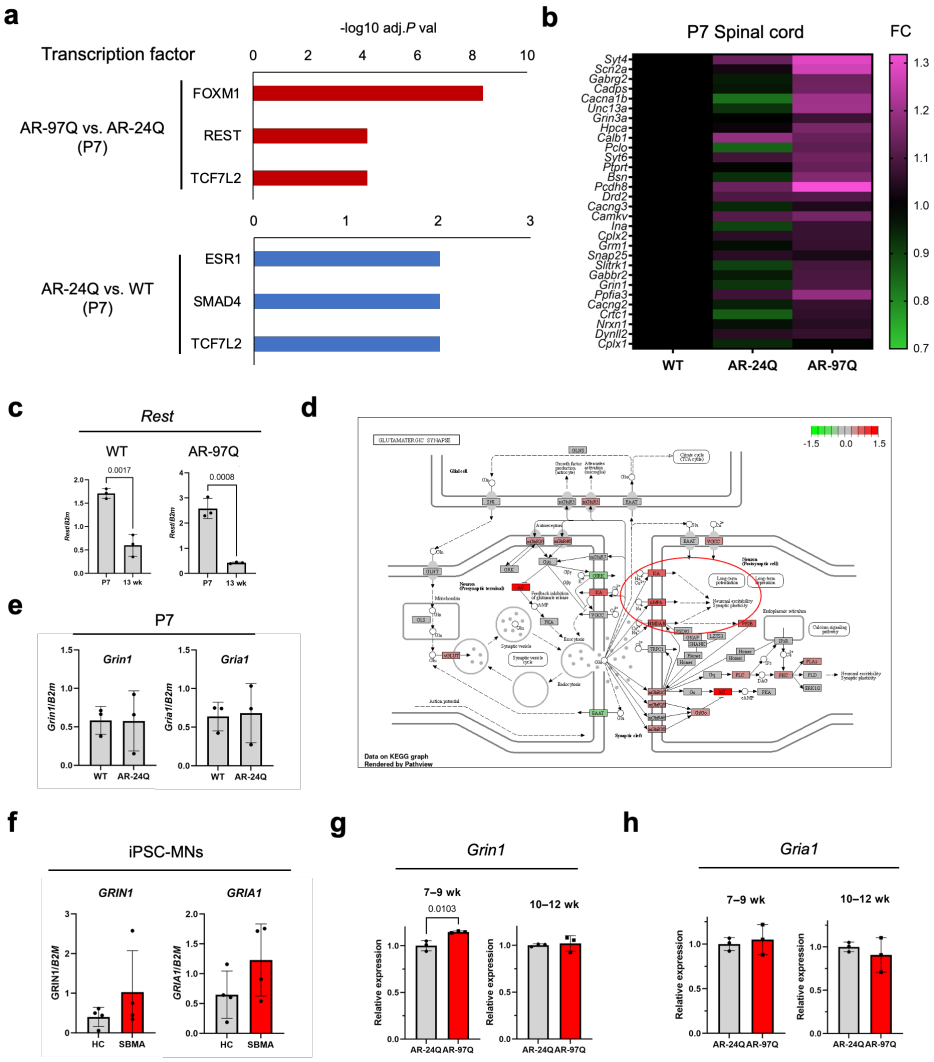

Supplementary Fig. 8 REST target glutamatergic synaptic genes are upregulated in the early stages of AR-97Q mice.

a GAGE analysis of RNA-seq data from spinal cord of AR-97Q, AR-24Q, and WT mice at P7 (n = 3 mice/group). The top three transcription factors in the category “ENCODE Transcription Factor Targets”, ranked by adjusted *P* value, are shown. **b** Heatmap of gene expression of REST target glutamatergic synapse in spinal cord of WT, AR-24Q, and AR-97Q mice at P7. **c** qPCR analysis of *Rest* mRNA normalized to *beta-2-microglobulin* (*B2m*) in the spinal cord at P7 and 13 weeks of age in male wild-type (WT) and AR-97Q mice (n = 3 mice/group). **d** KEGG pathway analysis using the RNA-seq data from the spinal cord of AR-97Q and WT mice at P7. Red and green represent up- and down-regulated genes in AR-97Q mice compared to WT mice, respectively. The analysis indicates the up-regulation of postsynaptic glutamate receptors, such as alpha-amino-3-hydroxy-5-methyl-4-isoxazole propionate (AMPA) and N-methyl-D-aspartate (NMDA) receptors, which lead to neuronal excitability (red circle). **e** qPCR analysis of *Grin1* and *Gria1* mRNA normalized to *B2m* in the spinal cord of male WT and AR-24Q mice at P7 (n = 3 mice/group). **f** qPCR analysis of *GRIN1* and *GRIA1* mRNA normalized to *B2M* in iPSC-derived purified motor neurons from healthy controls (HC) and SBMA patients (n = 4 iPSC lines/group). **g,h** Relative expression of *Grin1* (**g**) and *Gria1* (**h**) from the microarray data of AR-24Q and AR-97Q mice at 7–9 and 10–12 weeks of age (n = 3 mice/group). Data are presented as mean values +/- SD (**c,e,f–h**). Significance was tested by two-tailed unpaired *t*-test for the two group comparisons (**c,e,f–h**). Source data are provided as a Source Data file.

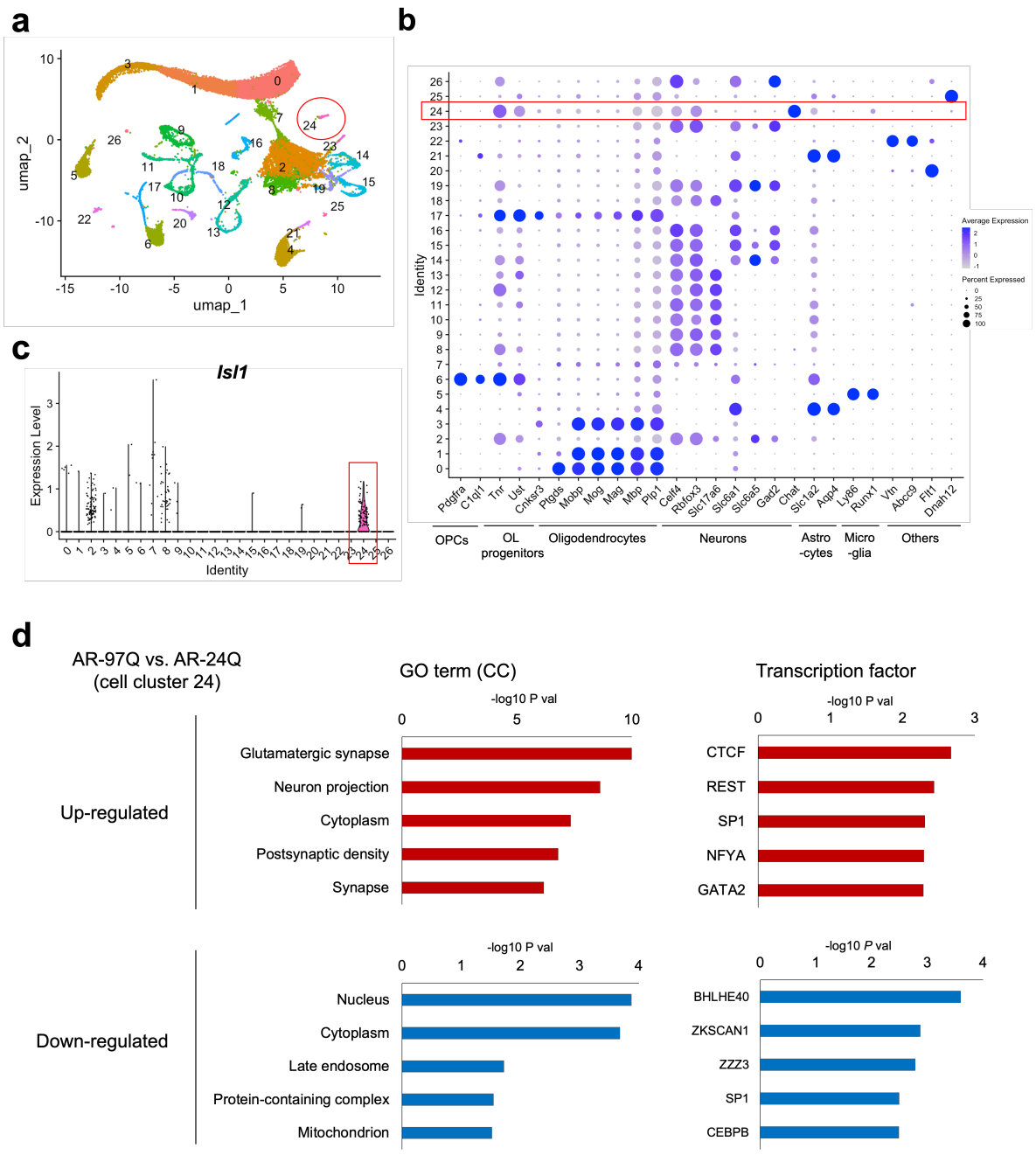

Supplementary Fig. 9. Single-nucleus RNA sequencing in the spinal cord of AR-97Q and AR-24Q mice.
a Uniform Manifold Approximation and Projection (UMAP) visualization of the dimension-reduced single-nucleus RNA sequencing (snRNA-seq) data from AR-97Q and AR-24Q mice at 8 weeks of age (n = 3 mice/group). **b** Dot plot showing the expression of known cell type-specific marker genes in cell clusters of the snRNA-seq data. **c** Expression levels of *Isl1* in each cell cluster. **d** Gene enrichment analysis of the top 100 up-regulated and down-regulated genes (ranked by absolute log fold change, $p < 0.05$) in the cell cluster 24 of AR-97Q and AR-24Q mice. A red circle (**a**) and squares (**b,c**) indicate the cell cluster expressing the *Chat* gene. Source data are provided as a Source Data file.

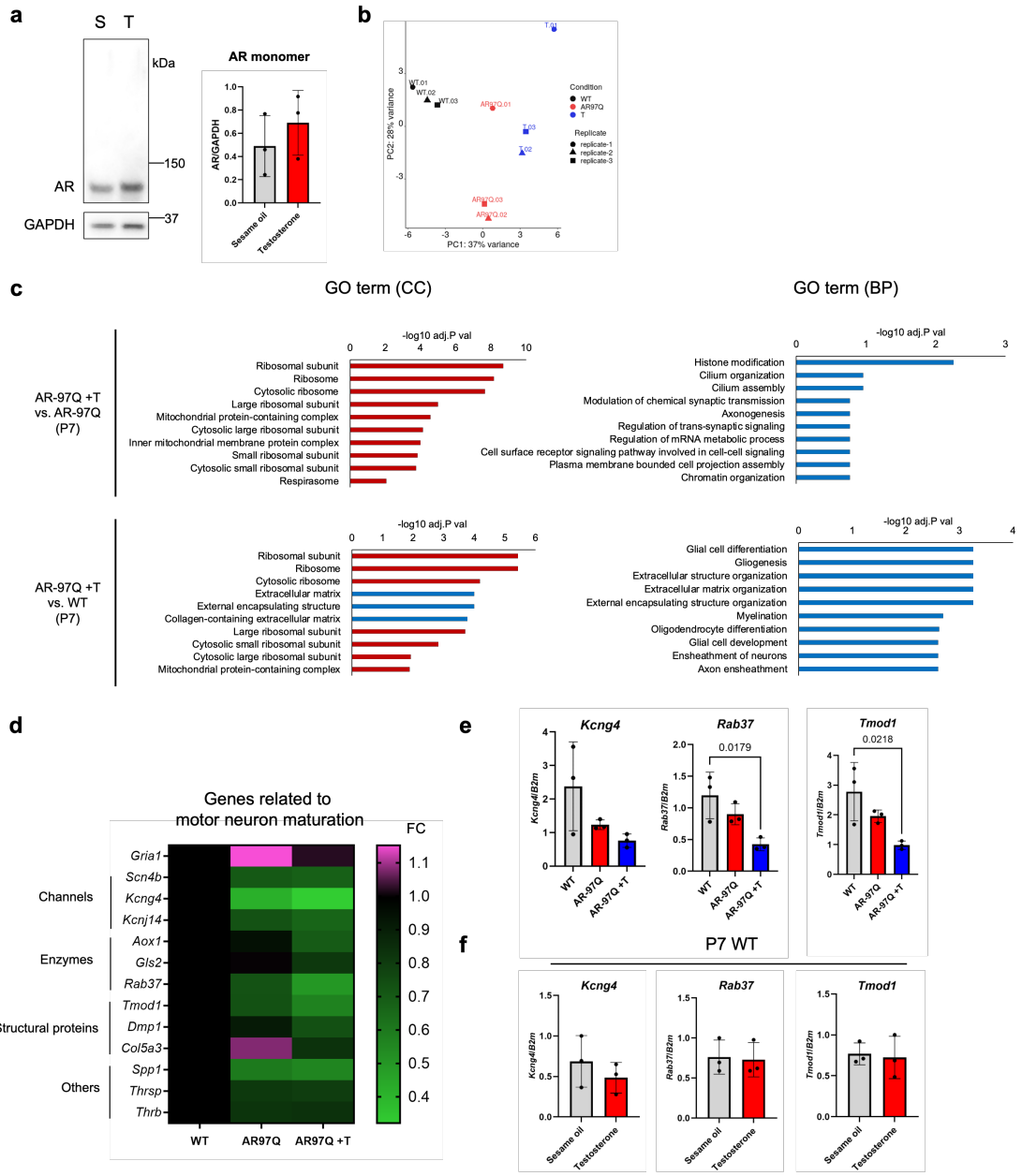

Supplementary Fig. 10 Neonatal testosterone administration inhibits genes related to motor neuron maturation.

a Immunoblots for human AR in the spinal cord of sesame oil (S)- or 20 μg of testosterone (T)-treated AR-97Q mice at P7 (n = 3 mice/group). **b** Principal component analysis of RNA-seq data from the spinal cord of wild-type (WT), AR-97Q, and T-treated AR-97Q mice at P7 (n = 3 mice/group). **c** Generally Applicable Gene-set Enrichment (GAGE) analysis of RNA-seq data in the categories “GO Cellular Component (CC)” and “GO Biological Process (BP)”. **d** Heatmap of gene expression related to motor neuron maturation in the spinal cord of WT, AR-97Q, and T-treated AR-97Q mice at P7. FC, fold change. **e** qPCR analysis of *Kcng4*, *Rab37*, and *Tmod1* normalized to *beta-2-microglobulin* (*B2m*) in the spinal cord of WT, AR-97Q, and T-treated AR-97Q at P7 (n = 3 mice/group). **f** qPCR analysis of *Kcng4*, *Rab37*, and *Tmod1* normalized to *B2m* in the spinal cord of sesame oil- or testosterone-treated WT mice (n = 3 mice/group). Data are presented as mean values +/- SD (**a,e,f**). Significance was tested by two-tailed unpaired t-test for the two group comparisons (**a,f**) or one-way ANOVA with Tukey’s post hoc test for the multiple group comparisons (**e**). Source data are provided as a Source Data file.

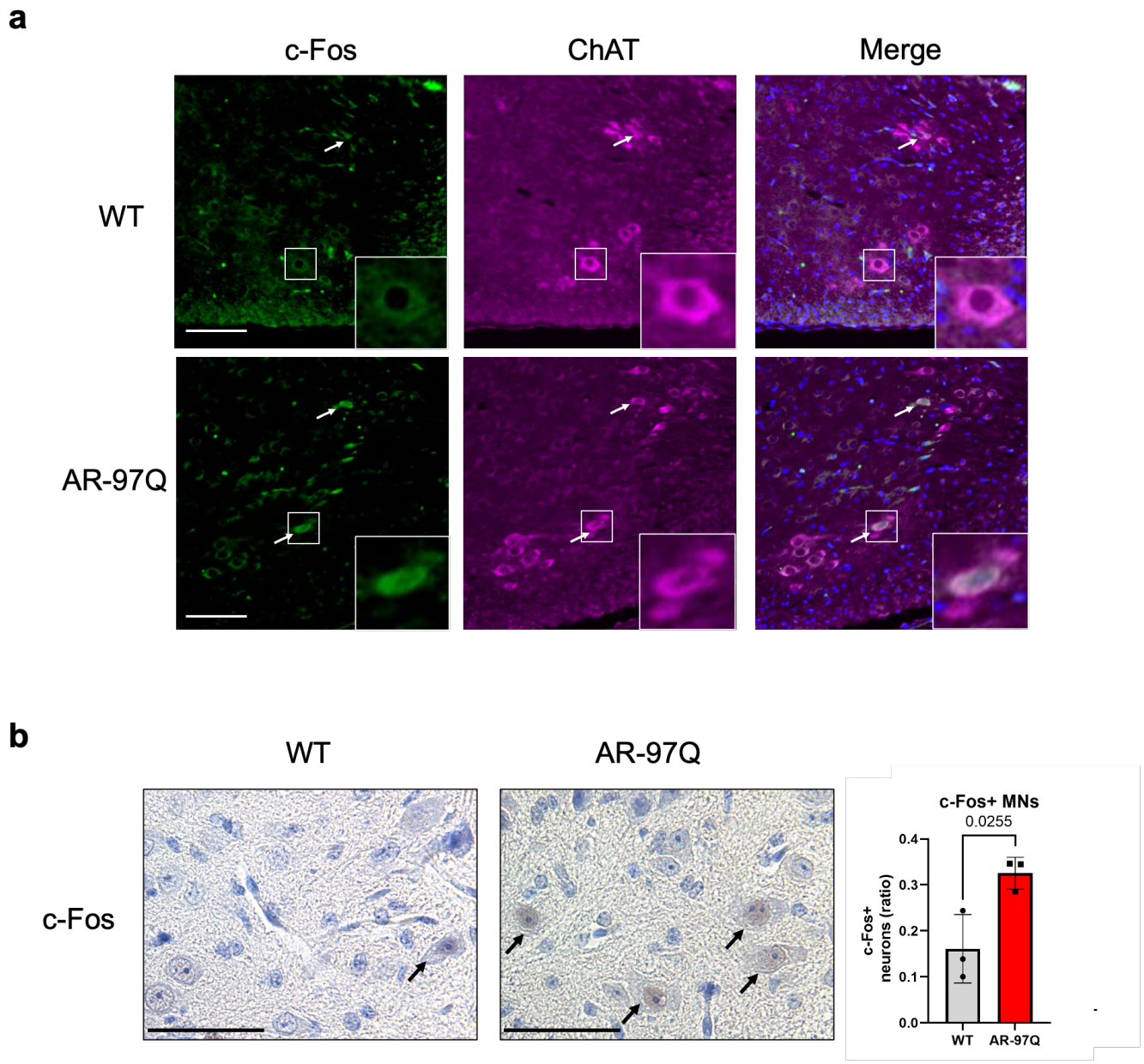

Supplementary Fig. 11 Increase in nuclear c-Fos-positive ratio in the motor neurons AR-97Q mice. **a** Immunofluorescence of c-Fos and choline acetyltransferase (ChAT) in the thoracic spinal cord of wild-type (WT) and AR-97Q mice at P7 (magnified images of Fig. 5a). Bar, 100 μm. **b** Anti-c-Fos immunostaining of motor neurons in the thoracic spinal cord of WT and AR-97Q mice at P7 (n = 3 mice/group) (WT, n = 97 neurons; AR-97Q, n = 123 neurons). Arrows indicate the nuclear c-Fos-positive (+) motor neurons. The number of c-Fos+ and total motor neurons in each mouse is provided in a Source Data file. Data are presented as mean values +/- SD. Significance was tested by two-tailed unpaired t-test. Source data are provided as a Source Data file.

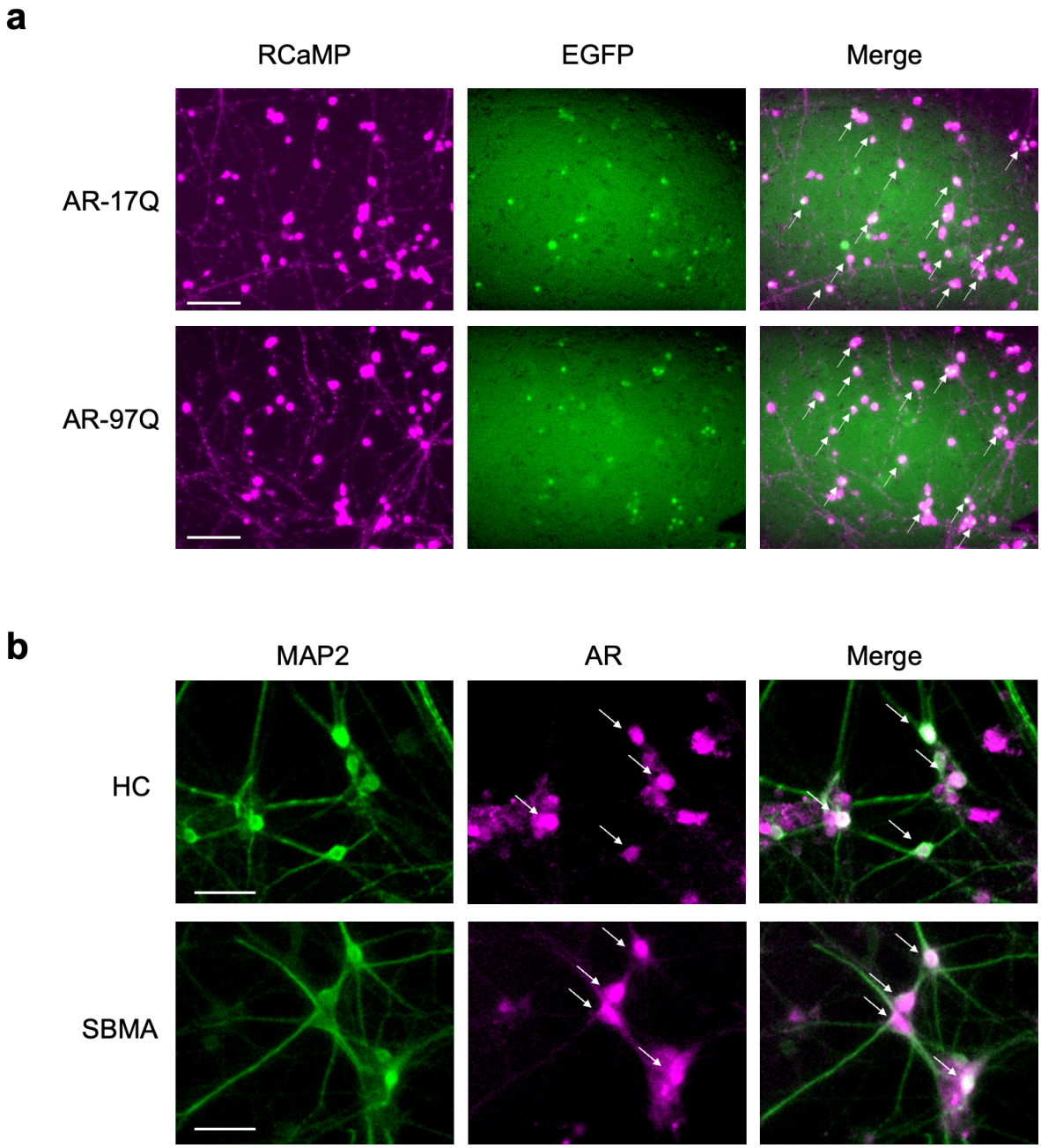

Supplementary Fig. 12 Nuclear localization of AR in iPSC-derived motor neurons.
a iPSC-derived motor neurons were infected with lentiviral RCaMP and EGFP-AR-17Q or 97Q and incubated with 10 nM DHT for 4 days. Live imaging of RCaMP and EGFP signals is shown. Bar, 100 μm. **b** Immunofluorescence of MAP2 and human AR in iPSC-derived motor neurons from SBMA patients and healthy controls (HC). Neurons were cultured with media containing 10 nM DHT for 4 days. Bar, 50 μm. Arrows indicate AR signal in the nucleus of IPSC-derived motor neurons.

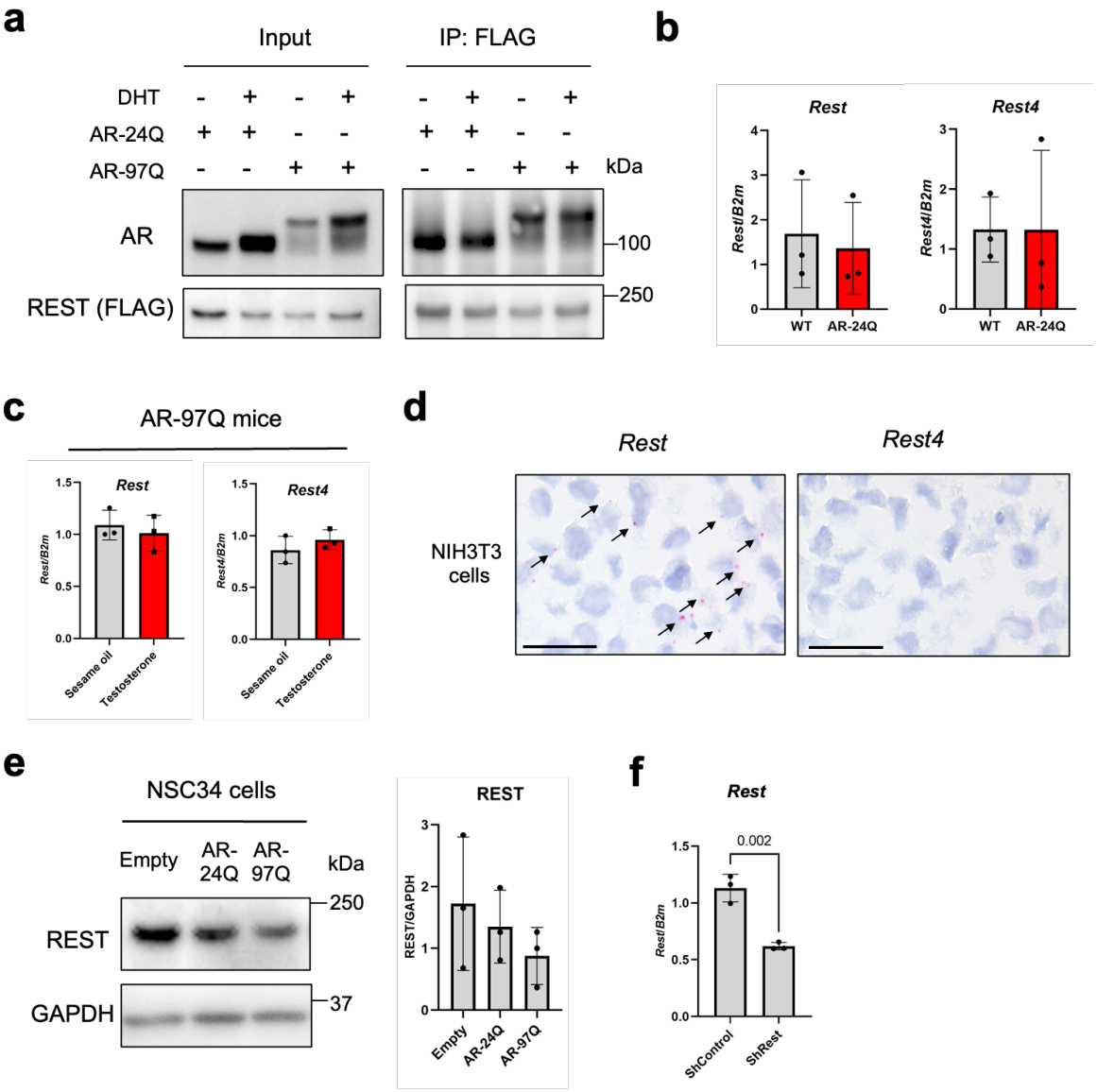

Supplementary Fig. 13 Interaction of REST with AR-24Q and AR-97Q and effects of AR-24Q and AR-97Q on the expression of *Rest* and *Rest4*.
a Immunoblots for AR and REST (FLAG) of input and immunoprecipitated (IP) lysates. REST-FLAG and AR-24Q or AR-97Q vector were co-transfected in NSC34 cells and incubated with or without 2 nM dihydrotestosterone (DHT) for 48 h. The cell lysates were immunoprecipitated with an anti-FLAG antibody. **b** PCR analysis of *Rest* and *Rest4* normalized to *beta-2-microglobulin* (*B2m*) in the spinal cord of WT and AR-24Q mice at P7 (n = 3 mice/group). **c** qPCR analysis of *Rest* and *Rest4* normalized to *B2m* in the spinal cord of sesame oil- or 20 μg of testosterone-treated AR-97Q mice at P7 (n = 3 mice/group). **d** *In situ* hybridization with the *Rest* and *Rest4* probe in NIH3T3 cells. Bar, 100 μm. Arrows indicate the signal of the transcripts. **e** Immunoblots for REST in NSC34 cells transfected with an empty, AR-24Q, or AR-97Q vector (n = 3 wells/group). **f** qPCR analysis of *Rest* normalized to *B2m* in NSC34 cells transfected with shRest and shControl (n = 3 wells/group). Data are presented as mean values +/- SD (**b,c,e,f**). Significance was tested by two-tailed unpaired *t*-test for the two group comparisons (**b,c,f**) and one-way ANOVA with Tukey's post hoc test for the three group comparisons (**e**). Source data are provided as a Source Data file.

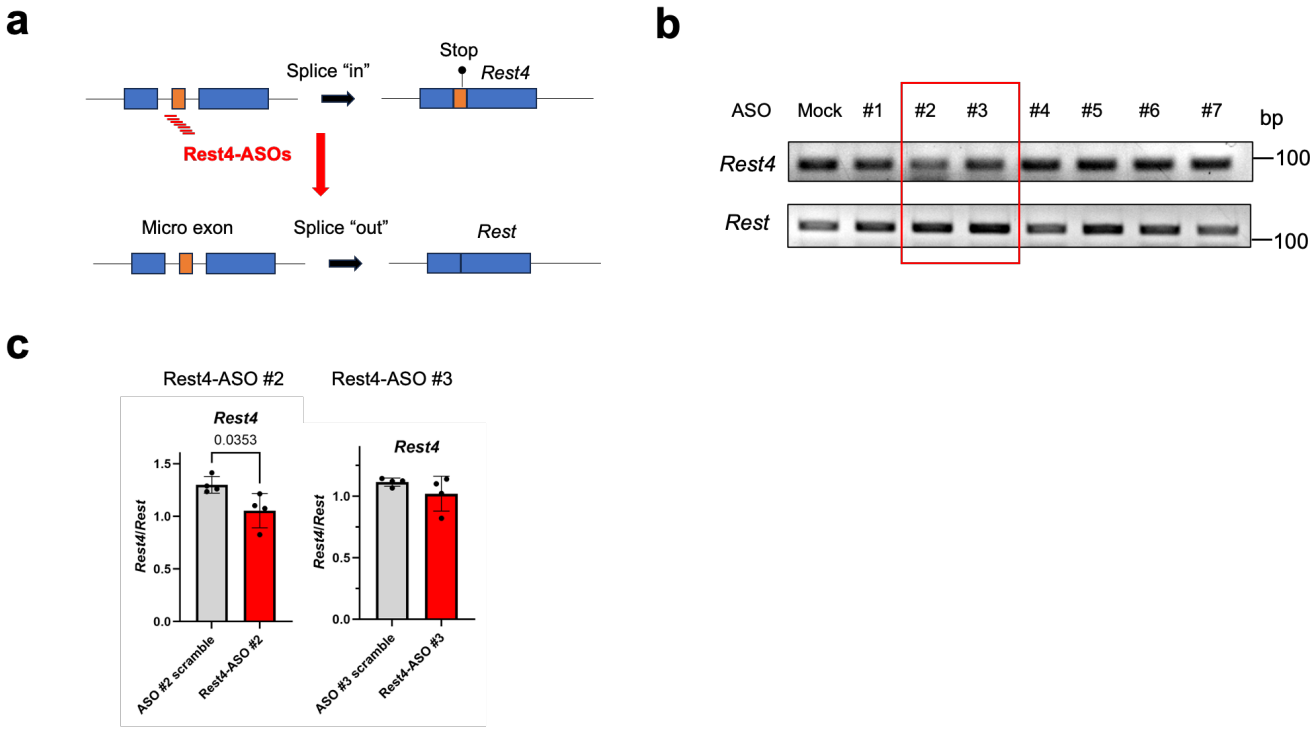

Supplementary Fig. 14 Screening of ASOs targeting a micro exon in *Rest4*.
a Scheme of a spice switching strategy using antisense oligonucleotides targeting a micro exon of *Rest4* (Rest4-ASOs). Rest4-ASOs inhibit micro exon inclusion, resulting in a decrease in *Rest4*/*Rest* ratio. **b** RT-PCR analysis of *Rest4* and *Rest* in NSC34 cells transfected with 50 nM of Rest4-ASOs (#1–7). **c** qPCR analysis of *Rest4* normalized to *Rest* in NSC34 cells transfected 50 nM of Rest4-ASO #2 or #3 compared to their scramble ASOs (n = 4 wells/group). Data are presented as mean values +/- SD. Significance was tested by two-tailed unpaired *t*-test for the two group comparisons. Source data are provided as a Source Data file.

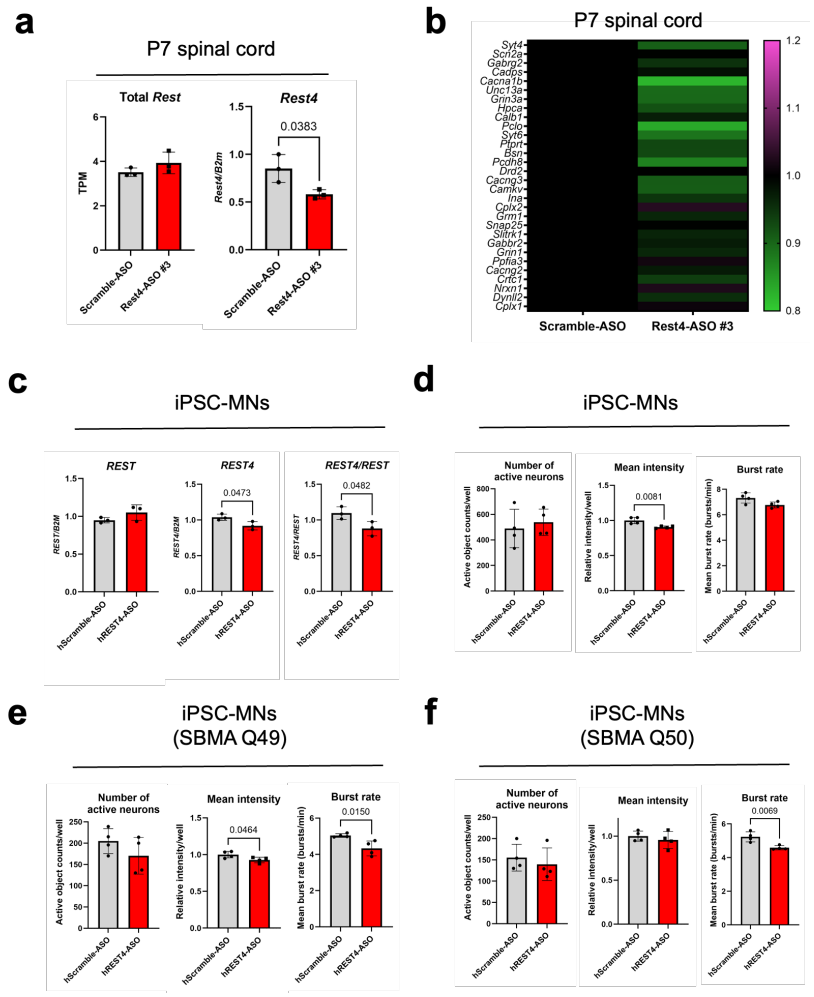

Supplementary Fig. 15 ASO-mediated splice switch from *REST4* to *REST* attenuates motor neuron hyperexcitability.
a Normalized expression of *Rest* from RNA-seq data and qPCR analysis of *Rest4* normalized to *beta-2-microglobulin* (*B2m*) in the spinal cord of Rest4-ASO #3 or Scramble-ASO-treated AR-97Q mice at P7 (n = 3 mice/group). TPM, transcript per million. **b** Heatmap of gene expression of REST target glutamatergic synapse in the spinal cord of Rest4-ASO #3 or Scramble-ASO-treated AR-97Q mice at P7. **c,d** iPSC-derived motor neurons (iPSC-MNs) were infected with lentiviral RCaMP and EGFP-AR-97Q at 1 day *in vitro* (DIV) , then cultured with 10 nM DHT and 1 μM hREST4-ASO or hScramble-ASO from 2 DIV for 4 days. Neuronal activity in the iPSC-MNs treated with hREST4-ASO or hScramble-ASO was measured for 3 minutes per well using Incucyte® SX5 system at DIV 6. Graphs show number of active neurons, mean intensity, and burst rate per well (n = 4 wells/group). qPCR analysis of *REST* and *REST4* normalized to *beta-2-microglobulin* (*B2M*), and the ratio of *REST4*/*REST* in the iPSC-MNs treated with hREST4-ASO or hScramble-ASO is shown in **c** (n = 3 wells/group). Numbers of active neurons, mean intensity, and burst rate per well are shown in **d** (n = 4 wells/group). **e,f** iPSC-MNs from SBMA patients harboring *AR* with 49 (**e**) or 50 (**f**) CAG repeats were infected with lentiviral RCaMP at 3 DIV, then cultured with 10 nM DHT and 1 μM hREST4-ASO or hScramble-ASO from 4 DIV for 4 days. Neuronal activity in the iPSC-MNs treated with hREST4-ASO or hScramble-ASO was measured for 3 minutes per well using Incucyte® SX5 system at DIV 8. Graphs show numbers of active neurons, mean intensity, and burst rate per well (n = 4 wells/group). Data are presented as mean values +/- SD (**a,c–f**). Significance was tested by two-tailed unpaired *t*-test for the two group comparisons (**a,c–f**). Source data are provided as a Source Data file.

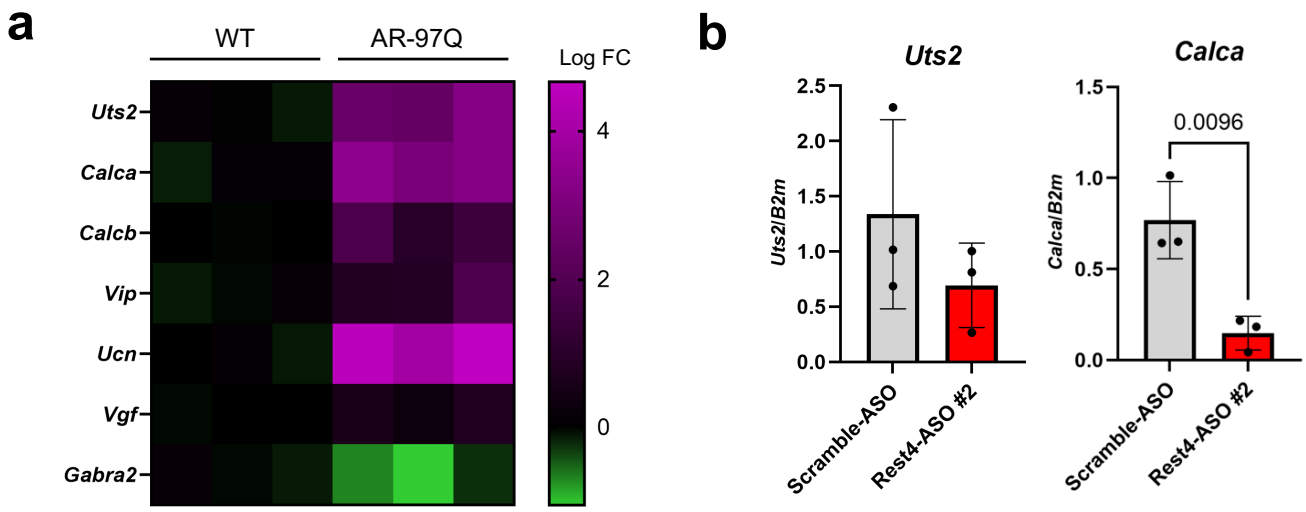

Supplementary Fig. 16 Early postnatal treatment reduces neuropeptide expression in later stages in AR-97Q mice.
a Heatmap of gene expression in the KEGG pathway “Neuroactive ligand receptor interaction” from RNA-seq data of the spinal cord of WT and AR-97Q mice at 13 weeks of age (n = 3 mice/group). **b** qPCR analyses of *Uts2* and *Calca* normalized to *beta-2-microglobulin* (*B2m*) in the spinal cord of Scramble-ASO or Rest4-ASO #2-injected AR-97Q mice at 13 weeks of age (n = 3 mice/group). Data are presented as mean values +/- SD. Significance was tested by two-tailed unpaired *t*-test for the two group comparisons. Source data are provided as a Source Data file.